PTL

DEVELOPMENTS IN ELECTRICAL CAPACITANCE TOMOGRAPHY

August 2001

SUMMARY

This is a copy of a keynote review paper presented by the author at the Second World Congress on Industrial Process Tomography in Hannover, Germany in August 2001. The paper is a review of the current status of Electrical Capacitance Tomography (ECT) and should provide a useful overview of the subject for both potential and existing users of ECT.

PROCESS TOMOGRAPHY LTD

86 Water Lane, Wilmslow, Cheshire. SK9 5BB United Kingdom.

Phone/Fax 01625-549021
(From outside UK +44-1625-549021)
email: ptl@tomography.com Web site: www.tomography.com

Registered in England No. 2908507. Registered Office 15, Croft Road, Wilmslow, Cheshire. SK9 6JJ United Kingdom.

Developments in Electrical Capacitance Tomography

Malcolm Byars

Process Tomography Ltd., 86, Water Lane, Wilmslow, Cheshire. SK9 5BB UK.
mbyars@tomography.com

ABSTRACT

Process Tomography Ltd has been supplying Electrical Capacitance Tomography (ECT) systems to the academic and industrial research sectors since 1995. This paper explains the basic techniques used in ECT and describes some recent developments in this technology

Keywords: Capacitance Tomography Permittivity Image Concentration

1 INTRODUCTION

Electrical Capacitance Tomography (ECT) is used to obtain information about the spatial distribution of a mixture of dielectric materials inside a vessel, by measuring the electrical capacitances between sets of electrodes placed around its periphery and converting them into an image showing the distribution of permittivity. ECT can be used with non-conducting materials such as plastics, hydrocarbons, sand or glass and is often used with mixtures of two different dielectric materials, as the permittivity distribution corresponds to the concentration distribution in this case. The image resolution achievable depends on the number of independent capacitance measurements, but is generally low. However, images can be generated at high frame rates, typically 100fps. Successful applications of ECT include imaging 2-phase liquid/gas mixtures in oil pipelines and solids/gas mixtures in fluidised beds and pneumatic conveying systems. Where the mixture is flowing along the vessel, measurements of the concentration distributions at two axial planes allow the velocity profile and the overall flow rate of the fluid to be found. In this paper we describe some of the developments in measurement hardware, software algorithms and physical models with which we have been associated over the last 6 years. Background information on ECT can be found in papers by Huang (1989) and Reinecke (1996).

2 MEASUREMENT SYSTEM CONFIGURATION

An ECT system consists of a capacitance sensor, measurement circuitry and a control computer. For imaging a single vessel type with a fixed cross-section and with a fixed electrode configuration, the measurement circuitry can be integrated into the sensor and the measurement circuits can be connected directly to the sensor electrodes. This simplifies the measurement of inter-electrode capacitances and is potentially a good design solution for standardised industrial sensors. However, most current applications for ECT are in the research sector, where it is preferable to have a standard capacitance measuring unit which can be used with a wide range of sensors. In this case, screened cables connect the sensor to the measurement circuitry, which must be able to measure very small inter-electrode capacitances, of the order of 10^{-15} F (1 fF), in the presence of much larger capacitances to earth of the order of 200,000 fF (mainly due to the screened cables). If the vessel wall is non-conducting, electrodes can be located inside, within or outside the wall as shown in figure 1. However, if the tube wall is a conductor, internal electrodes must be used. The convention we use to identify electrodes is to number them anticlockwise, starting at the electrode at or just before 3 o'clock.

The number of sensor electrodes that can be used depends on the range of values of inter-electrode capacitances and the upper and lower measurement limits of the capacitance measurement circuit. The capacitance values when the sensor contains air are referred to as "standing capacitances" and their relative values are shown in figure 2 for a 12-electrode circular sensor with internal electrodes. Sequential electrodes are referred to as adjacent electrodes, and have the largest standing capacitances, while diagonally opposing electrodes (opposite electrodes) have the smallest capacitances. Because of the wide range of these capacitances, they are usually normalised to lie within a standard range of values, as described in section 6. As the number of electrodes increases, the electrode surface area per unit axial length decreases and the inter-electrode capacitances also

decrease. When the smallest of these capacitances (for opposite electrodes), reaches the lowest value that can be measured reliably by the capacitance circuitry, the number of electrodes, and hence the image resolution, can only be increased further by increasing the axial lengths of the electrodes. However, these lengths cannot be increased indefinitely because the standing capacitances between pairs of adjacent electrodes will also increase and the measurement circuitry will saturate or overload once the highest capacitance measurement threshold is exceeded.

3 CAPACITANCE MEASUREMENT PROTOCOLS

Many different ECT measurement protocols are possible (Reinecke, 1994), as capacitances can be measured between many combinations of groups of electrodes (which effectively become new "virtual electrodes"). Most work to-date with circular vessels has used the simplest arrangement (which we refer to as protocol 1) where capacitances are measured between single pairs of electrodes. The measurement sequence for protocol 1 involves applying an alternating voltage from a low-impedance supply to one (source) electrode. The remaining (detector) electrodes are all held at zero (virtual ground) potential and the currents which flow into these detector electrodes (and which are proportional to the inter-electrode capacitances) are measured. A second electrode is then selected as the source electrode and the sequence is repeated until all possible electrode pair capacitances have been measured. This generates M independent inter-electrode capacitance measurements, where:

$$M = E.(E - 1)/2 \quad (1)$$

and E is the number of electrodes located around the circumference. For example for E = 12, M = 66. As the measurements for a single frame of data are made sequentially, the capacitance data within the frame will be collected at different times and there will be some skewing of the data. Interpolation techniques can be used to de-skew this data if this effect is likely to produce significant errors.

Other possible protocols involve grouping electrodes and exciting them in pairs (protocol 2) and triplets (protocol 3) etc. The formula for the number of independent measurements for grouped electrodes is :

$$M = (E).(E - (2P - 1)) / 2 \quad (2)$$

where P (the protocol number) is the number of electrodes which are grouped together. The advantage of using these more complex protocols is that they can generate a larger number of independent measurements for a given electrode size and capacitance measurement sensitivity than the simple single-pair protocol 1. Improved image resolution is therefore achievable, although at the expense of the maximum image frame rate, which falls as the protocol number or number of electrodes increases.

4 CAPACITANCE SENSORS

ECT can be used with vessels of any cross-section, but most work to-date has used circular geometries. For a sensor with internal electrodes, the components of capacitance due to the electric field inside the sensor will always increase in proportion to the material permittivity when a higher permittivity material is introduced inside the sensor. However for sensors with external electrodes, the permittivity of the wall causes non-linear changes in capacitance, which may increase or decrease depending on the wall thickness and the permittivities of the sensor wall and contents. In general, ECT sensors with external electrodes are easier to design and fabricate than internal electrode sensors and they are also non-invasive.

Axial resolution and overall measurement sensitivity can be improved by the use of driven axial guard electrodes, located either side of the measurement electrodes, as shown in the flexible laminate design of figure 3. These electrodes are excited at the same electrical potentials as the associated measurement electrode and prevent the electric field from being diverted to earth at the ends of the measurement electrodes. For large diameter vessels, axial guard electrodes are normally an essential requirement to ensure that the capacitances between opposing electrodes are measurable.

With the current state of capacitance measurement technology, it is possible to measure capacitance changes between 2 unearthed electrodes of 0.2 fF in the presence of stray capacitance to earth of 200pF at a rate of 2000 measurements per second. This sets a practical lower design limit on the capacitance between any pair of electrodes of around 10fF, which translates to measurement electrodes of minimum axial length 3.5cm for an 8 electrode sensor or 7 cm for a 12 electrode sensor. These dimensions assume that effective driven axial guards are used. For this condition to be met, the sum of the lengths of the axial guard and the measurement electrodes must equal or exceed the sensor diameter.

5 SENSOR FABRICATION

The required electrode pattern can be designed using CAD software and the electrodes fabricated using photolithographic techniques from a flexible copper-coated laminate, which is then wrapped around the outside of an insulating tube to form the sensor. Part of a design for an 8-electrode single plane sensor with driven axial guards is illustrated in figure 3, which shows earthed screening tracks between the sets of electrodes (to reduce the adjacent electrode capacitances) together with earthed areas at the ends of the sensor (to allow the cable screens to be terminated). Coaxial leads (with a maximum length of 2m to minimise capacitance to ground) are connected to the electrodes and an earthed screen is located around the sensor to exclude any external signals. Discharge resistors (typically 1 MOhm) must be connected between each electrode and the cable screen to ensure that no static charge can build up on the electrodes and connecting leads, otherwise damage may occur when the sensor is connected to the capacitance measurement circuit. These basic techniques can be used to construct static or sliding sensors with internal or external electrodes. More complex fabrication techniques are needed for sensors for operation at elevated temperatures and pressures.

6 NORMALISATION OF MEASUREMENTS AND SENSOR CALIBRATION

When a mixture of 2 dielectric materials is to be imaged, ECT systems are normally calibrated by measuring two reference sets of inter-electrode capacitances, C_L and C_H with the sensor filled with the lower and higher permittivity materials in turn. All subsequent capacitance values C_M are then normalised to have values C_N between zero (when the sensor is filled with the lower permittivity material) and 1 (when filled with the higher permittivity material) according to the formula:

$$C_N = (C_M - C_L) / (C_H - C_L) \quad (3)$$

The pixel values in the permittivity image are similarly normalised, so that they have the value 0 for the lower permittivity material and 1 when the sensor is filled with the higher permittivity material.

7 CAPACITANCE/PERMITTIVITY/CONCENTRATION MODELS

The relationship between the permittivity distribution and the capacitance measured between a pair of electrodes must be considered carefully if accurate permittivity/concentration images are to be obtained. If the two dielectric materials exist as discrete stratified permittivity layers between the two electrodes, then two component capacitances, each due to one of the dielectric materials, and effectively connected in parallel, will exist between the electrodes. The sum of these capacitances will therefore accurately reflect the relative proportions of the 2 materials present. However, if the materials exist as alternating bands of permittivity between the electrodes, the capacitances measured between the electrodes will be constituted from component capacitances which are effectively connected in series. In this case, the reciprocal rule must be used to obtain the component permittivities and concentration from the measured capacitances. If there is a combination of these two basic material distributions, more complex relationships, such as the method described by Maxwell, must be used to define the permittivity/ concentration/ capacitance relationships. It is therefore very important to use the correct permittivity model (parallel/series/Maxwell etc) if accurate concentration values are to be obtained from the permittivity image. Further information on capacitance/ permittivity models (including Maxwell's method) is given in the paper by Yang and Byars (1999).

8 FORMAT OF PERMITTIVITY IMAGES

The permittivity distribution of a mixture of two fluids is often displayed as a series of normalised pixels located on either a (32 x 32) or (64 x 64) square pixel grid, using an appropriate colour scale to indicate the normalised pixel permittivity (as shown, for example, in figure 6). This uses a graduated blue/green/red colour scale, where pixel values corresponding to the lower permittivity material used for calibration have the value zero and are shown in blue, while pixels corresponding to the higher permittivity material have the value 1 and are shown in red. The normalised permittivity distribution corresponds to the fractional concentration distribution of the higher permittivity material. If the sensor cross-section is circular, this circular contour must be projected onto the square grid containing typically 1024 pixels. Some of the pixels will lie outside the vessel circumference and the image is therefore formed from those pixels that lie inside the vessel. A typical arrangement which is commonly used is shown in figure 4, where the circular image is constructed using 812 of the available 1024 pixels.

9 IMAGE RECONSTRUCTION

The resolution of an ECT permittivity image is limited by the number of independent measurements that can be made and this relationship can be considered to be an example of spatial filtering, as shown in figure 5. The resolution limit is difficult to define mathematically, but a simple engineering estimate can be made by assuming that the number of independent measurements M corresponds to a similar number of discrete regions inside the sensor. If we assume that the angular resolution is equal to the number of electrodes E, then the radial resolution will equal M/E. For protocol 1 and a 12 electrode sensor, this gives a radial resolution limit of 5.5. For protocol 2 and 24 electrodes, this figure increases to 10.5.

It is not possible to obtain a unique solution for each image pixel when the number of pixels in the image exceeds the number of capacitance measurements. Furthermore, image distortion can occur because ECT is an inherently soft-field imaging method (the electric field is distorted by the material distribution inside the sensor). However, in many cases, the contrast between the permittivities of the materials inside the sensor is small, resulting in only limited image distortion. This allows approximate linear algorithms to be used to relate the capacitance measurements to the pixel values in the image and vice-versa. The method which has been used with greatest success to-date is known as Linear Back Projection (LBP), and is based on the solution of a set of forward and reverse (or inverse) transforms.

The forward transform is a matrix equation which relates the set of inter-electrode capacitance measurements **C** to the set of pixel permittivity values **K.** This transform assumes that the measured inter-electrode capacitances resulting from any arbitrary permittivity distribution **K** inside the sensor will be identical to those obtained by summing the component capacitance increases which occur when each pixel has its defined permittivity, with all other pixels values set to zero. This forward transform is defined in equation 4, where bold characters represent matrices :

$$\mathbf{C = S.K} \tag{4}$$

C is an (M x 1) dimensioned matrix containing the set of M inter-electrode pair capacitances (where M is typically 66 for a 12-electrode sensor or 28 for an 8-electrode sensor for protocol 1).

K is an (N x 1) dimensioned matrix (where N is 1024 for a 32 x 32 grid) containing the set of N pixel permittivity values which describe the permittivity distribution inside the sensor (the permittivity image).

S is the forward transform, usually known as the sensor Sensitivity Matrix. **S** has dimensions (M x N) and consists of M sets (or maps) of N (typically 1024) coefficients, (1 map for for each of the M capacitance-pairs), where the coefficients represent the relative change in capacitance of each capacitance pair when an identical change is made to the permittivity of each of the N (1024) pixels in turn.

In principle, once the set of inter-electrode capacitances **C** have been measured, the permittivity distribution **K** can be obtained from these measurements using an inverse transform **Q** as follows.

$$\mathbf{K = Q.C} \tag{5}$$

Q is a matrix with dimensions (N x M) and, in principle, is simply the inverse of the matrix **S**. However, it is only possible to find the true inverse of a square matrix (where M = N). In physical terms, this is confirmation that it is not possible to obtain the individual values of a large number of pixels (eg 1024) from a smaller number of capacitance measurements (eg 66). As an exact inverse matrix does not exist, an approximate matrix must be used. The LBP algorithm uses the transpose of the sensitivity matrix, **S'** which has the dimensions (N x M) and this is justified by the following reasoning: Although we have no means of knowing which pixels have contributed to the capacitance measured between any specific electrode-pair, we know from the sensitivity matrix **S** that certain pixels have more effect than others on this capacitance. Consequently, we allocate component values to each pixel proportional to the product of the electrode-pair capacitance and the pixel sensitivity coefficient for this electrode-pair. This process is repeated for each electrode-pair capacitance in turn and the component values obtained for each pixel are summed for the complete range of electrode-pairs. This simple algorithm produces approximate, but very blurred permittivity images, and a typical image, for a dielectric tube inside a 12-electrode sensor, is shown in figure 8. The LBP algorithm acts as a spatial filter with a lower cut-off frequency than that of the fundamental filter (as shown in figure 5) and produces sub-optimal images from a given set of input data.

10 THE SENSITIVITY MATRIX

The forward transform (sensitivity matrix) must be calculated (or measured) for each individual sensor as a separate exercise prior to using the sensor with an ECT system. One method for calculating the sensitivity coefficient S of a pixel for an electrode-pair (i-j) is based on the use of equation 6.

$$S = \int_A \mathbf{E}_i \,.\, \mathbf{E}_j \,.\, dA \qquad (6)$$

where $\mathbf{E}_i$ is the electric field inside the sensor when one electrode of the pair i is excited as a source electrode, $\mathbf{E}_j$ is the electric field when electrode j is excited as a source electrode and the dot product of the two electric field vectors $\mathbf{E}_i$ and $\mathbf{E}_j$ is integrated over the area A of the pixel. The set of sensitivity coefficients for each electrode-pair is known as the sensitivity map for that pair. For circular sensors with either internal or external electrodes, it is possible to derive an analytical expression for the electric fields and in this case, the sensitivity coefficients (and also the electrode capacitances) can be calculated accurately. For more complex geometries, numerical methods can be used to calculate the sensitivity coefficients. It is normally only necessary to calculate a few primary sensitivity maps for the unique geometrical electrode pairings, as all of the other maps can be derived from these by reflection or rotation. A set of primary maps for an 8-electrode sensor operating under protocol 1 is shown in figure 7.

11 ITERATIVE METHODS FOR IMPROVING IMAGE QUALITY

It is possible to improve the image resolution and accuracy to values much closer to the theoretical limit shown in figure 5 by the use of iterative techniques. The idea is to use equations 4 and 5 alternately to progressively correct the pixel values, and is based on the assumption that the forward transform (equation 4) is reasonably accurate if the field distortion is low but that the inverse transform (equation 5) may be very inaccurate. This technique is conceptually similar to the practice of correcting the distortion of an imperfect amplifier by the use of negative feedback.

The method operates as follows: The set of capacitances $\mathbf{C_1}$ for one image frame are measured and a set of initial pixel values $\mathbf{K_1}$ are calculated using (the inaccurate) equation 5. These approximate permittivity values $\mathbf{K_1}$ are then used to back-calculate a set of capacitances $\mathbf{C_2}$ using (the accurate) equation 4. A set of error capacitances $\Delta\mathbf{C} = (\mathbf{C_2} - \mathbf{C_1})$ are calculated and used to generate a set of error permittivities $\Delta\mathbf{K}$ using equation 5. These error permittivities are then used to correct the previous set of permittivities to generate a new set of pixel values $\mathbf{K_2}$, where $\mathbf{K_2} = (\mathbf{K_1} - \Delta\mathbf{K})$. These new permittivities $\mathbf{K_2}$ are then used to calculate a new set of capacitances $\mathbf{C_2}$ and the sequence is iterated until the permittivity values converge to the correct solution. A number of additional steps are possible, including truncating the image pixels to lie within the known calibration range at each iteration and applying gain and truncation factors to the error capacitances. However, it is important to check that the permittivity values converge in order to ensure a valid solution. Experience shows that this method can produce images of good resolution, close to the theoretical maximum achievable with a given measurement protocol and number of electrodes. Sample images are shown in figures 6 and 9.

12 SINGLE-STEP METHODS FOR IMPROVING IMAGE QUALITY

Although the iterative method produces good images, it cannot be used on-line because of the time taken to carry out the relatively large number of iterations required to produce the image. It is possible to develop better inverse transforms for **Q** by using more advanced mathematical concepts for deriving approximate inverses of matrices. Two examples are methods developed by Landweber and Tikhonov, where the inverse matrix **Q** for each of these methods is defined as follows:

Landweber transform:

$$\mathbf{Q_L = V \,.\, F\,(\,W,}\ t,\ R\ \mathbf{)\,.\,U'} \tag{7}$$

where: **V, W** and **U** are the matrices obtained by applying the Single Value Decomposition (SVD) process to the sensitivity matrix **S , F** is the **SVD** filter function matrix, **U'** is the transpose of **U** and

$$f = (\,(1 - (\,1 - L.\,w\,)^{R}\,)\,/\,w \tag{8}$$

where: f is one element of the filter matrix **F,** w is one element of the diagonal matrix **W,** L is the Landweber transform parameter and R is the number of iterations.

Tikhonov transform:

$$\mathbf{Q_T = S' \,.\, (\,S \,.\, S' + t \,.\, I\,)^{-1}} \tag{9}$$

where: **S** is the sensitivity matrix, **S'** is the transpose sensitivity matrix, t is the Tikhonov transform factor, and **I** is the identity matrix.

Some insight into the mechanism of operation can be seen from figure 10, which shows the Landweber transform plotted as an equivalent set of primary sensitivity maps. By comparing figures 7 and 10, it is clear that the Landweber transforms have far more structure, and produce more detailed images from the same capacitance data, as shown in figure 11, although they also produce some spurious artefacts in the image. These can be reduced, while further improving the image, by carrying out a small number of iterations using the appropriate inverse transform in place of the transpose sensitivity matrix, as the image in figure 12, obtained after only 5 iterations, illustrates. The attraction of these techniques is that they are fast enough for use on-line.

13 FLOW MEASUREMENT

In principle, ECT can be used to measure the flow of a fluid mixture by measuring the concentration profiles **K** at two measurement planes simultaneously and by using correlation techniques to extract the velocity profile **V**. The flow profile is the product **K.V** and the flow rate is obtained by integrating the flow profile over the cross sectional area. In practice, the frame rates achievable with ECT at present limit the use of this technique to situations where the fluid mixture is moving relatively slowly.

14 CONCLUDING REMARKS

ECT is a useful measurement tool which continues to be the subject of on-going research to improve it's effectiveness. The development of new measurement hardware capable of operating with multi-electrode protocols and higher frame rates, together with improved image reconstruction techniques offers the prospects of higher image resolution and accuracy and the potential for using ECT in flow measurement applications. The excitation methods used in ECT can also be used to image partially-conducting solutions, and a dual-mode ECT/ERT measuring system is therefore a future possibility. Finally, we would like to acknowledge the considerable help we have received from Dr Bill Lionheart of UMIST (with various aspects of image reconstruction described in this paper) and also from John Pendleton, (John Pendleton Associates), who wrote the sensitivity map and image generation software used to produce the results for this paper.

15 REFERENCES

Huang S.M. et al., (1989), Tomographic imaging of two-component flow using capacitance sensors, J. Phys. E: Sci. Instrum. 22, pp 173-177.

Reinecke N. and Mewes D., (1994), Resolution enhancement for multi-electrode capacitance sensors, in Proc: Process Tomography, A strategy for Industrial Exploitation, Bergen Norway, pp50 - 61

Reinecke N. and Mewes D., (1996), Recent Developments and industrial/research applications of capacitance tomography, Meas. Sci. Technol. 7 pp 233-246

Yang W.Q. and Byars M., (1999) An improved normalisation approach for electrical capacitance tomography, in Proc : 1st World Congress on Industrial Proc. Tomography, Buxton, UK pp 215-218.

16 FIGURES

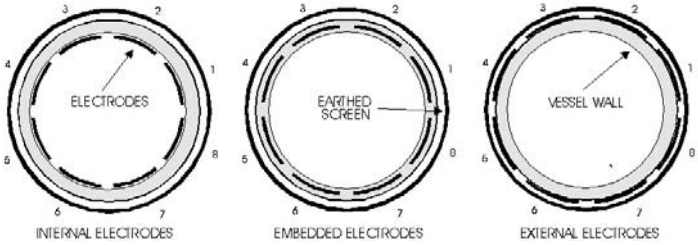

Figure 1 Circular sensor electrode configurations

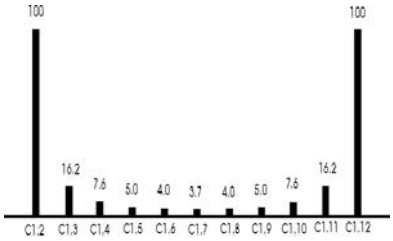

Figure 2. Inter-electrode capacitances

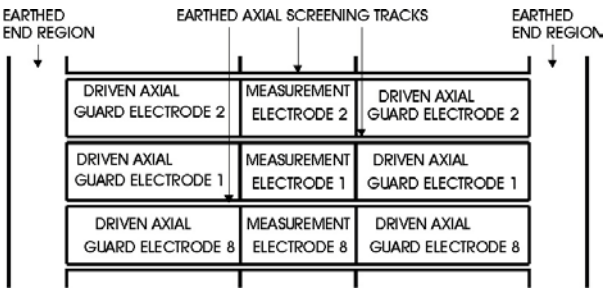

Figure 3. Partial PCB layout for an 8-electrode single-plane sensor

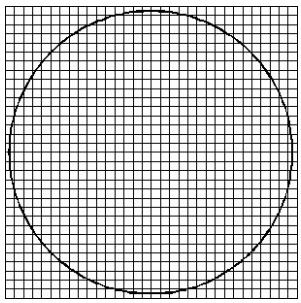

Figure 4. Image pixel grid

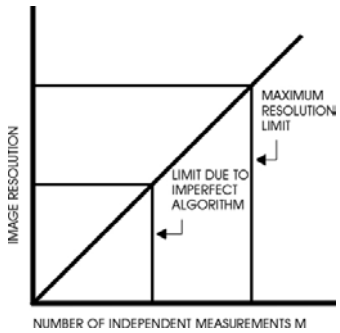

Figure 5. Spatial filter resolution limits.

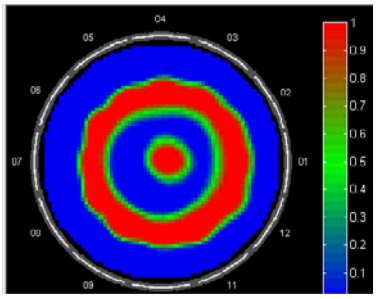

Figure 6. Permittivity image of a Dielectric rod inside a dielectric tube

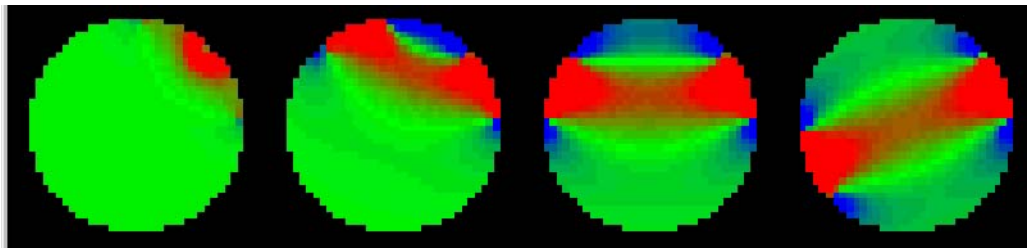

Figure 7. Primary Sensitivity Maps for an 8-electrode sensor

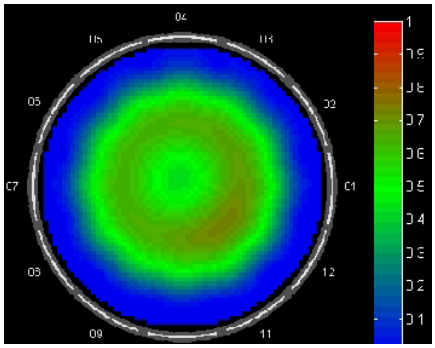

Figure 8. 64 x 64 pixel LBP image for Plastic tube inside 12-electrode sensor

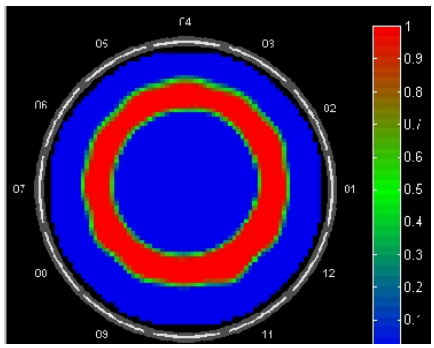

Figure 9. Image from same capacitance data after 100 iterations

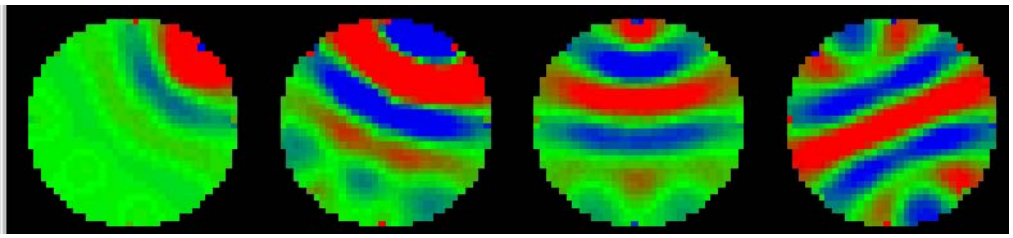

Figure 10. Landweber transforms for an 8-electrode sensor (L = 0.01, R = 100)

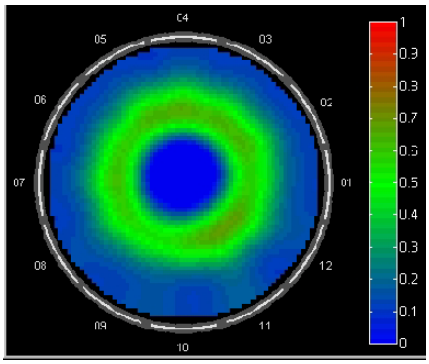

Figure 11. Image from same data using Landweber Transform (L = 0.01, R = 100).

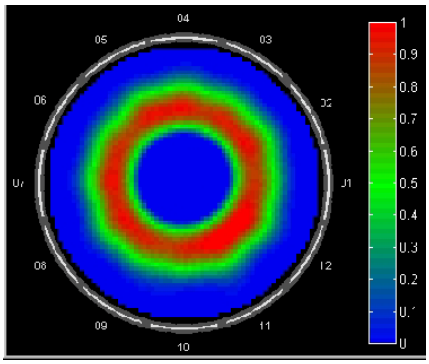

Figure 12. Image from same data using 5 Iterations of Landweber transform

Notes: **Permittivity images: Colour scale progresses from zero (blue) through green to (1) red. Sensitivity and transform maps: Maps show relative sensitivities on a compressed colour scale, where: Blue = -ve, green = zero, red = +ve sensitivity regions.**